

CONF-960772-23

UCRL-JC-123380

Extents of Alkane Combustion During Rapid Compression
Leading to Single and Two Stage Ignition

A. Cox, J. F. Griffiths, C. Mohamed,
H. Curran, W. J. Pitz, C. K. Westbrook

RECEIVED
AUG 16 1996
OSTI

This paper was prepared for submittal to the
Twenty-Sixth Symposium on Combustion
Napoli, Italy
July 28-August 2, 1996

February 1996

MASTER



Lawrence
Livermore
National
Laboratory

This is a preprint of a paper intended for publication in a journal or proceedings. Since changes may be made before publication, this preprint is made available with the understanding that it will not be cited or reproduced without the permission of the author.

DISTRIBUTION OF THIS DOCUMENT IS UNLIMITED

DISCLAIMER

This document was prepared as an account of work sponsored by an agency of the United States Government. Neither the United States Government nor the University of California nor any of their employees, makes any warranty, express or implied, or assumes any legal liability or responsibility for the accuracy, completeness, or usefulness of any information, apparatus, product, or process disclosed, or represents that its use would not infringe privately owned rights. Reference herein to any specific commercial product, process, or service by trade name, trademark, manufacturer, or otherwise, does not necessarily constitute or imply its endorsement, recommendation, or favoring by the United States Government or the University of California. The views and opinions of authors expressed herein do not necessarily state or reflect those of the United States Government or the University of California, and shall not be used for advertising or product endorsement purposes.

DISCLAIMER

**Portions of this document may be illegible
in electronic image products. Images are
produced from the best available original
document.**

EXTENTS OF ALKANE COMBUSTION DURING RAPID COMPRESSION LEADING TO SINGLE AND TWO STAGE IGNITION

A. Cox, J.F. Griffiths and C. Mohamed
School of Chemistry,
The University,
Leeds LS2 9JT, UK

and

H. Curran, W.J. Pitz and C.K. Westbrook
Lawrence Livermore National Laboratory,
Livermore, CA 94550, USA

The Twenty-Sixth Symposium on Combustion
Università Federico II
Napoli, Campi Phlegraei, ITALY
July 28 - August 2, 1996

ABSTRACT

Extents of reactant consumption have been measured during the course of spontaneous ignition following rapid compression of n-pentane and n-heptane and also of PRF 60 (n-heptane + i-octane, 2,2,4 trimethylpentane) in stoichiometric mixtures with air. Compressed gas temperatures of 720-750 K and 845 - 875 K were studied at reactant densities of 131 mol m^{-3} . At the lower gas temperature there was no evidence of reactant consumption during the course of the compression stroke. Two-stage ignition occurred at these temperatures, but only modest proportions of n-pentane were consumed during the first stage (< 15%) whereas about 40% of n-heptane reacted under the same conditions. At the higher compressed gas temperature the oxidation of n-pentane began only after the piston had stopped, whereas more than 30% of the n-heptane had already been consumed in the final stage of the compression stroke. The behaviour of the PRF 60 mixture differed somewhat from that of n-pentane despite the similarity of the research octane numbers. Although there was a preferential oxidation of n-heptane at $T_C = 850 \text{ K}$, which persisted throughout the early development of spontaneous ignition during the post-compression period, oxidation of both components of the PRF 60 mixture began before the piston had stopped. Numerical simulations of the spontaneous ignition under conditions resembling those of the rapid compression experiments show that the predicted reactivity from detailed kinetics are consistent with the observed features. Insights into the kinetic interactions that give rise to the relative reactivities of the primary reference fuel components are established.

INTRODUCTION

The spontaneous ignition (or autoignition) characteristics of hydrocarbons have been of interest to chemists and engineers for many decades. The current interest relates predominantly to combustion in reciprocating engines, and the occurrence of knock in spark ignition (s.i.) engines in particular. One effect of mechanical compression is that quite considerable reaction and

accompanying heat release may occur during the compression stroke itself. The extent to which this occurs is governed by reactivity of the fuel and the pressure and temperature to which the reactant charge is finally compressed. Such effects may have a bearing on the spontaneous oxidation processes which eventually lead to end-gas autoignition in s. i. engines, and are taken into account in numerical simulations of combustion in engines [1].

In previous studies in a rapid compression machine it was shown that during the combustion of n-C₇H₁₆ and n-C₆H₁₄ at compressed gas temperatures above 750 K exothermic reaction could occur in the final stages of piston motion at a sufficient rate that there was an enhancement of the gas temperature beyond that reached by adiabatic compression alone [2]. In some circumstances, the features of a two-stage ignition of the more reactive fuels were masked by the coincidence of the first stage with the end of compression. Little or no oxidation occurred during the compression stroke when less reactive fuels, such as n-C₅H₁₂ or n-C₄H₁₀, were involved.

In this work we report experimental measurement of the extents of reactant consumption during the development of spontaneous ignition of alkanes in a rapid compression machine, with particular emphasis on reactivity during the compression stroke. Three fuels studied, in stoichiometric mixtures in air, were n-C₅H₁₀, n-C₇H₁₆ and the PRF 60 mixture 0.4 n-C₇H₁₆ + 0.6 i-C₈H₁₈ (2.2.4 trimethylpentane). The binary mixture was investigated in order to establish whether or not there is any selective consumption of the more reactive component (n-C₇H₁₆), and PRF 60 was chosen because its research octane number is close to that of n-C₅H₁₂ (RON = 62.5).

Over the last decade there has been a considerable development of numerical approaches to the prediction of spontaneous ignition phenomena through the simulation of events from thermokinetic models representing the detailed chemistry and its associated heat release [1,3].

Ignition delays have been a primary focus of attention [3], but increasingly there has been a move to test the validity of the models against detailed chemical information about the formation of intermediate and final molecular products [1, 4-7]. Thus it is both timely and opportune to apply numerical modelling to the experimental results reported here for reactant consumption. As is inevitable in the development stage, some aspects of the thermokinetic modelling are very satisfactory but others require further consideration. The reward for developing a kinetic understanding through numerical methods is the power to gain quantitative insights into the interactions, at the elementary reaction level, that govern the global behaviour. The prediction of the performance of complex fuel mixtures also becomes a possibility, and an initial investigation is presented here.

A spatial uniformity of temperature and concentration of species is assumed in the kinetic analysis in order to restrict the numerical integration to that of ordinary differential equations, as is normally the case, since the coupling of detailed kinetic models to complex fluid mechanical models that represent the gas dynamics associated with the experimental systems has not yet been fully mastered. However, spatial inhomogeneities of temperature and concentration are known to exist to varying extents throughout the course of piston motion of rapid compression machines and throughout the post compression interval in which spontaneous ignition develops fully [8 -10].

EXPERIMENTAL AND NUMERICAL METHODS

Experimental studies

Full details of the apparatus and experimental procedures have been described previously [2, 11 - 14]. In summary, fuel vapour was premixed with 'air' consisting of 21% oxygen and a 79% composite of non-reactive components comprising argon or nitrogen. The proportions of the inerts were varied to alter the overall heat capacity of each mixture, and hence the ratio C_p/C_v ($=\gamma$). Thus a range of compressed gas temperatures could be covered at a fixed compression ratio of the machine

(CR = 11.00 \pm 0.15 : 1) Experiments were performed at the compressed gas temperatures of 720 - 750 K and 845 - 875 K. The hydrocarbons used were of analytical or research grade. Mixtures, stored in a Pyrex glass vacuum line, were transferred at an initial pressure of 33.3 kPa to the combustion chamber and then compressed into a cylindrical combustion chamber by a piston which was driven by compressed air and which stopped at "top dead centre", the stroke taking 22 ms. The cylinder and combustion chamber temperature (T_i) were maintained at 323 - 348 (\pm 1) K. The compressed gas density was $131.0 \pm 1.5 \text{ mol m}^{-3}$ in all experiments.

Pressure-time data during the compression and throughout the post compression period were measured by Kistler transducer and recorded digitally on a pc at a sampling rate of 200 μs per point via an A/D converter, 200 ms in total. Chemiluminescent emission accompanying reaction was measured by photomultiplier in selected experiments (Thorn EMI 9924B). The ignition delay (t_i), measured from the pressure records, was defined as the time from the end of compression to the maximum rate of pressure rise in ignition. In general the ignition delays, measured in 3 - 6 experiments at each reactant composition and compressed gas temperature, were reproducible to \pm 2.0 ms at long durations and \pm 1.0 ms at short durations. The compressed gas temperature, T_c , was derived from the measured pressures at the start and end of compression, p_i and p_c , and taking into account the temperature dependence of γ , using the relationship

$$\int \frac{\gamma}{T_i(\gamma-1)} d\ln T = \ln(p_c/p_i)$$

In order to analyse the reactant and product compositions at intermediate stages, the reaction was quenched by the bursting of a diaphragm (99% Al, 0.1 mm thickness) in the end-wall of the combustion chamber, which formed the cylinder head. This was followed by the expansion of

the reactant mixture into a hemispherical dump tank (1.5 dm^3), as described previously [11]. The time at which the diaphragm burst was controlled by a time delayed signal generated at a threshold pressure during the compression stroke which was used to actuate an electromagnetically driven needle. The condensable components were then pumped to a cold trap coupled to the vacuum line. In order to obtain time dependent profiles for the reactant consumption, many experiments were performed under the same compression conditions, but with quenching after different intervals. The results for each set of experimental conditions were obtained from a number of separate mixtures made up to the same composition. The scatter of the experimental results is attributable to these factors.

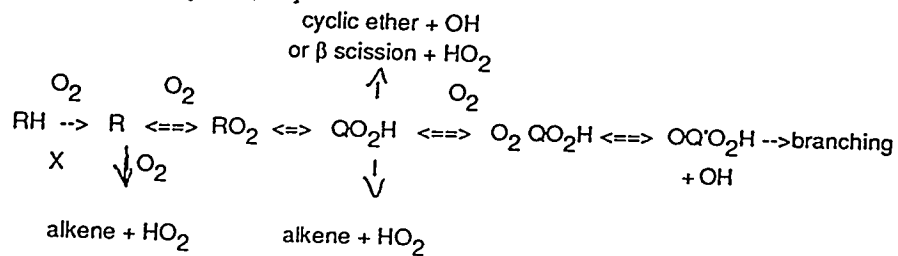
A standardising procedure was required in order to relate the extents of reaction in a series of experiments. The sealed cold trap was allowed to warm to laboratory temperature and a standard volume of n- C_4H_{10} was injected into the trap via a septum cap and, after complete mixing, a gaseous sample was withdrawn from the trap via a microsyringe and injected into the analytical system. A separation of the mixture was performed by gas chromatography (Carlo Erbe) on a fused silica, Poraplot Q-coated, capillary column (25 m x 0.32 mm) and a quantitative analysis was obtained from the integrated peak areas of the eluting compounds. The proportions of the fuel remaining in each experiment were obtained from a determination of the peak area of the primary fuel peak relative to that of n-butane. This result was then normalised to a constant peak area which represented the n-butane signal. The extents of reaction were expressed as a percentage relative to the amount of reactant measured following compression under non-reactive conditions. Product compositions were not analysed in the present work.

Numerical Analysis and Kinetic models

The numerical modelling calculations were carried out using the HCT program [15], which solves the coupled non-linear differential equations for conservation of mass, momentum, energy

and each chemical species, in finite difference form. The compression stroke was simulated *ab initio* from the initial conditions and reactant compositions for the experimental results, adiabatic conditions being assumed. The reaction mechanism included about 3500 elementary chemical reactions with their reverse steps. This reaction mechanism includes submechanisms for oxidation of C₁ - C₈ hydrocarbon species, validated against a variety of experimental data for ignition and combustion environments [1]. These mechanisms include reactions governed by formation and consumption of alkylperoxy radical species that are appropriate to low temperatures.

Distinctions were made between the rates of abstraction of H atoms from primary, secondary and tertiary sites in each alkane and between equilibrium constants for addition of molecular oxygen to different types of alkyl radicals. The most significant, subsequent reactions of the alkylperoxy radicals ($C_nH_{2n+1}OO$) so formed are their isomerisations via internal H atom abstraction, at rates which depend primarily on the type of C - H bond being broken and the ring strain energy of the intermediate transition state [7]. The many distinct $C_nH_{2n}OOH$ (QOOH) radicals can decompose thermally, producing hydroxyl radicals and cyclic ethers. Depending on their specific structure, some QOOH radicals can also decompose to produce stable alkene or oxygenated species and HO_2 or OH radicals. All of these reactions lead to chain propagation. The only reactions of alkylperoxy radicals which lead to vigorous chain branching involve addition of a second oxygen molecule, producing ketohydroperoxide intermediates which then decompose to produce radicals. Rates and equilibrium constants for these reaction paths have been developed in recent studies [1, 6, 7]. The kinetic structure to represent alkane oxidation at low temperatures may be summarised as follows [7, 16, 17].



RESULTS

Combustion at $T_c = 720 - 750 K$

Pressure change and fractional extents of reactant consumption versus time that were measured during the spontaneous ignition of n-C₅H₁₂ and n-C₇H₁₆ at $\phi = 1$ are shown in Figs 1 and 2. The numerically derived, fractional extent of fuel consumption as a function of time is also given. The pressure - time records begin at 2 ms before the end of piston motion and continue throughout the development of ignition. The pressure record shown in Fig. 1 also includes the sharp fall which occurred when the quenching diaphragm was punctured. This illustrates the rate of expansion of the products into the dump tank. In this case the pressure did not reach the maximum that was normally attained at ignition (> 3.0 MPa) since the reaction was quenched.

Both n-C₅H₁₂ and n-C₇H₁₆ exhibited a two-stage ignition in this compressed gas temperature range, which is evident both in the pressure record and in the accompanying chemiluminescent emission from the reaction (Figs. 1 and 2). The first stage of two-stage ignition is interpreted as the development from the end of compression to the point of inflection in the pressure rise [4, 5, 18]. There was very little or negligible consumption of either reactant before the piston had stopped but, whereas nearly 40% of the n-C₇H₁₆ had reacted by the end of the first stage (Fig. 2), less than 15% of the n-C₅H₁₂ had been consumed (Fig. 1).

There was a particularly sharp acceleration in the rate of consumption of n-C₅H₁₂ during the development of the second stage but, even so, only 80% of it had been consumed at the highest quenching pressure (1.9 MPa). The discrepancies of experimental results in Fig. 1, which imply that there is a lower extent of conversion at a later time during the development of the hot stage

of ignition, arise from the small variations in ignition delay from one experiment to another. Similar features are to be seen in other results reported here. The rate of change of fuel concentration during the development of the hot stage of n-C₇H₁₆ ignition was rather less marked than that of n-C₅H₁₂ since only 50% of the fuel remained subsequent to the first stage of reaction and then only 80% had been consumed at the highest quenching pressure.

The computed first stage and overall ignition delays for n-C₅H₁₂ and n-C₇H₁₆ combustion at these compressed gas temperatures are in excellent agreement with the experimental results. The model results show a negligible extent of reaction at the end of compression, as in the experiments. The model gives a prediction of greater extents of reaction of both fuels during the first stage than was observed in the experiments, however, with 40% and 60% for n-C₅H₁₂ and n-C₇H₁₆ respectively, at the end of this period.

Combustion at $T_c = 845 - 875\text{ K}$

The experimental and numerical reactant consumption profiles and the experimental pressure - time records for the combustion of n-C₅H₁₂ and n-C₇H₁₆, and also for a PRF 60 reactant mixture are shown in Figs 3 - 5. The ignition delay for the spontaneous ignition of n-C₅H₁₂ at a compressed gas temperature of $853 \pm 4\text{ K}$ was $16 \pm 1\text{ ms}$, which is similar to that at the lower compressed gas temperature, but it developed in a single stage (Fig. 3). There was no measurable reactant consumption before the piston motion stopped, and the extent of fuel consumption increased smoothly throughout the ignition delay interval. Nevertheless, only 50% had reacted even to within 2 ms of attainment of the peak pressure in ignition.

The combustion of n-C₇H₁₆ at a high compressed gas temperature ($T_c > 850\text{ K}$) was also a

single stage ignition, with ignition delay similar to that at $T_C = 750$ K, but the profile for reactant consumption was quite different from the measured profile for n-C₅H₁₂ (Fig. 4). Reactant consumption began more than 1 ms before the piston had stopped (at which the mean gas temperature was calculated to be below 750 K) and 38±5 % had been consumed by "top dead centre". Subsequently, there was only a relatively small increase in the amount of fuel consumed during the early part of the post compression period, and an increase in reactant consumption beyond 60% occurred only in the final stage of ignition. Also shown in Fig. 4 is the pressure record from a non-reactive composition of the same heat capacity as the reactive mixture. A lower compressed gas pressure is reached and there is a departure of the reactive curve from the non-reactive curve, which begins at about 1 ms before the piston has stopped. This relates to the time at which exothermic oxidation of n-C₇H₁₆ begins to augment the gas temperature during the compression stroke. The decay in pressure following the end of compression in the non-reactive case arises from heat loss to the chamber wall.

Although the predicted ignition delay for n-C₅H₁₂ from the numerical study was longer than the measured time, the extent of reaction followed an identical profile to that measured experimentally in the early stages (Fig. 3). Departures from the experimental profile emerged at calculated gas temperatures in excess of 920 K. The simulated overall ignition delay for n-C₇H₁₆ ignition was also slightly longer than that measured experimentally, but the extents of reactant consumption throughout most of the ignition delay were in very good agreement with the experimental results (Fig. 4). The extent of reaction that was predicted to have occurred before the piston had stopped was 33%, although it began closer to the end of compression than in the experiments.

The experimental and numerical results obtained from a single stage ignition of the binary

mixture $0.6 \text{ i-C}_8\text{H}_{18} + 0.4 \text{ n-C}_7\text{H}_{16}$ (PRF 60) at a compressed gas temperature of $864 \pm 4 \text{ K}$ are shown in Fig. 5 ($t_i = 32 \pm 2 \text{ ms}$). The consumption of both reactants began whilst the piston was still moving, but more $\text{n-C}_7\text{H}_{16}$ than $\text{i-C}_8\text{H}_{18}$ had reacted (50% versus 45%) by the time the piston stopped. Very little of either fuel was further consumed during the early part of the post-compression period, and the rate of heat generation during this interval was sufficiently low that the heat loss became a dominant influence. This is the cause of the decay in the experimental pressure record during the ignition delay. The discrepancy between the predicted and measured ignition delays is attributable in part to the assumption of adiabaticity in the calculations. This must also affect the reactant consumption profiles, but there are qualitative differences that have to be reconciled in some other way. Consumption of $\text{n-C}_7\text{H}_{16}$ was predicted to begin ($> 0.1\%$) just at the end of compression, followed by reaction of $\text{i-C}_8\text{H}_{18}$ about 1 ms later.

Supplementary measurements were also made in a reactive mixture containing only the $\text{i-C}_8\text{H}_{18}$ component (that is, $\text{i-C}_8\text{H}_{18}$ at $\phi = 0.6$) but of similar heat capacity to that of the PRF 60 mixture. Ignition of this composition did not occur following compression to 130 mol m^{-3} and $T_c = 860 \text{ K}$, but nevertheless approximately 20% of the reactant had been consumed before the end of compression and there was a gradual increase to 30% during a 10 ms interval of the post-compression period (Fig. 6). These experiments have not yet been analysed numerically.

DISCUSSION

Adiabaticity, heat loss and spatial temperature variations

Compression at the piston speeds used in the Leeds machine has been shown previously to be virtually adiabatic [2]. Thus assumptions of adiabaticity of the system and spatial uniformity of

temperature and concentration in the numerical modelling during the compression stroke is very satisfactory. However, spatial temperature variations develop within the combustion chamber during the post-compression period as a result of heat transport to the combustion chamber walls. The heat loss rates are highest just after compression ceases because the residual gas motion is greatest at this stage [9]. Thereafter the rate of heat loss decreases as the gas motion decays.

Adiabaticity was assumed in the calculations also throughout the post compression period. The simulation of ignition delay thus implies that the behaviour is dominated by conditions in the adiabatic core [19], but there are complexities of the interaction between the kinetics and a non-homogeneous temperature field in a temperature range where a negative temperature dependence of reaction rate exists [9, 10]. In general, the calculated extent of reaction at any time after the end of compression, with adiabatic conditions assumed, may be expected to be an overestimate relative to an experimental measurement which is obtained from the amount of reactant remaining within a non-uniform temperature regime comprising cooler regions surrounding an adiabatic core. The relationship in a negative temperature dependent region is a special circumstance that still requires a deeper understanding.

The heat loss rate throughout the post compression period may be characterised by a Newtonian heat transfer coefficient in a zero-dimensional numerical model [20]. However, its application can adversely affect the predicted reactivity because there is a highly non-linear response of the chemical kinetics to reactant temperature. Rates and extents of reaction cannot be averaged in a simple way throughout a combustion chamber in which spatial variations in temperature exist.

Extents of reaction in single and two-stage ignition and during compression

The greater reactivity of n-C₇H₁₆ over that of n-C₅H₁₂ at T_c ~ 750 K is not only reflected

in the shorter ignition delay but also it is manifest directly in the extents of reaction measured in the first stage of two-stage ignition. In previous rapid compression studies, Fish *et al* [21] measured approximately 25% consumption of 2-methylpentane during the first stage of two-stage ignition at $T_C = 808$ K. For n-C₄H₁₀, Minetti *et al* [4] showed that there was only 10-15% reactant consumption during the first stage of two-stage ignition at $T_C = 708$ K whereas approximately 25% consumption of n-C₇H₁₆ occurred during the first stage of its two-stage ignition at $T_C = 667$ K [5].

of two-stage ignition
The slow development of the first stage may be

attributed to the chain-thermal interaction in which the thermal feedback is required to accelerate the degenerate branching route [17]. Its rate is controlled largely by the activation energies associated with the RO₂/QO₂H isomerisations, but the properties of each of the other steps play a part in the quantitative behaviour. The more vigorous acceleration in rate of n-C₇H₁₆ consumption in the first stage of two-stage ignition, which was found both experimentally and numerically, testifies to its much more facile chain branching route than that of n-C₅H₁₂. The limit on chain branching is set by the displacement of the R/RO₂ equilibrium towards dissociation as the reactant temperature increases beyond 850 K. This is the primary kinetic origin of the negative temperature dependence of reaction rate since the main (non-branching) propagation is taken up with relatively low exothermicity by HO₂ radicals [17].

There are both chemical and thermal consequences of oxidation in the final stages of

compression. The thermal contribution is an augmentation of the gas temperature beyond that which would be reached by rapid compression alone, and the effect can be seen in the difference between the pressures attained under reactive and non-reactive conditions (Fig. 4). The temperature increase predicted in the numerical simulations is 30 K.

The difference in reactivity shown by n-C₇H₁₆ and n-C₅H₁₂ also accounts for the ability of n-C₇H₁₆ to react during the compression stroke when compression occurs beyond T_C = 800 K. Although thermal feedback has some effect on gas temperature, the reactant temperature is forced through the most reactive temperature regime (750 - 800 K) at a rate determined by the compression stroke. At a piston speed of 12 m s⁻¹ in the Leeds rapid compression machine there is sufficient time for n-C₇H₁₆ to react. Although this is not the case for n-C₅H₁₂ under the present conditions, it could be so for n-C₅H₁₂ or other fuels of similar reactivity at higher reactant densities.

Schlieren imaging of spontaneous ignition in the rapid compression machine shows that the hot stage often begins at a single centre, and the bulk of the reactants are consumed in a propagating combustion wave before other centres are initiated [22]. Consequently, a quenching of reaction on the rising pressure profile of the final stage of ignition gives rise to a product composition drawn from segregated burned gas and partially oxidised reactants. Thus, the measured extents of reaction in the late stage of reaction cannot be expected to match quantitatively the numerically predicted results, as seen especially in Figs. 3 and 4. The end of the experimental ignition delay is also likely to be affected by this inhomogeneous development. So the inevitable difference of the ignition delay predicted in a zero dimensional analysis should not be interpreted as inaccuracies in the kinetic model. Nor are kinetic parameter adjustments appropriate to compensate for the difference.

The measured ignition delay of a PRF 60 mixture at $T_C = 864 \pm 6$ K and $\phi = 130 \text{ mol m}^{-3}$, $t_i = 32 \pm 2$ ms, is longer than that for n-C₅H₁₂ (RON = 62.5) under similar conditions. Nevertheless, by contrast to n-C₅H₁₂, reaction had already begun before the piston had stopped, 50 ± 4 % of n-C₇H₁₆ and 45 ± 4 % of i-C₈H₁₈ having been consumed. The absolute amount of n-C₇H₁₆ that had been consumed by the end of compression of this mixture was about half that which had reacted during the combustion of n-C₇H₁₆ alone at a similar compressed gas temperature (Fig. 4).

Although there are significant qualitative differences in the form of the predicted profiles for the PRF 60 mixture which still have to be addressed, the predicted ratio of the fractional extents of reaction throughout the ignition delay at temperatures below 900 K, $d(\% \text{nC}_7\text{H}_{16})/d(\% \text{iC}_8\text{H}_{18})$, is 1.24 \pm 0.03, which is in excellent agreement with the experimental measurements at the end of compression (1.11 \pm 0.12). It follows that the relative concentration of alkyl radicals, $d[\text{C}_7\text{H}_{15}]/d[\text{C}_8\text{H}_{17}]$, generated in the PRF 60 mixture in this environment is (40/60) \times 1.24 (or 1.11) = 0.83 + 0.02 (or 0.74 \pm 0.08). This ratio is consistent with an almost exclusive role of H atom abstraction by OH radicals, as can be derived from the ratio for $k(\text{n-C}_7\text{H}_{16} + \text{OH}) / k(\text{i-C}_8\text{H}_{18} + \text{OH})$ in the range 800 - 900 K, taking into account the numbers of primary, secondary or tertiary C - H bonds in each alkane and the respective Arrhenius parameters [23]. The relatively weak selectivity in favour of C₈H₁₇ radical formation in the PRF 60 mixture would shift very substantially towards C₈H₁₇ radical formation in PRF mixtures containing higher proportions of i-C₈H₁₈.

Oxidation of $n\text{-C}_7\text{H}_{16}$ generates a rate of chain branching which is much more intense than that of $i\text{-C}_8\text{H}_{18}$, since the structure of the C_7H_{15} radicals leads to higher rates of peroxy radical isomerisation [1], ultimately causing chain branching from ketohydroperoxide decomposition. Increasing fractions of $i\text{-C}_8\text{H}_{18}$ in PRF mixtures would, therefore, reduce the overall rate of combustion since the rate of chain branching would decrease. This is apparent in a qualitative way in a comparison between the reactivity at high compressed gas temperatures between $n\text{-C}_7\text{H}_{16}$ and PRF 60 (Figs. 4 and 5) and between PRF 60 and $i\text{-C}_8\text{H}_{18}$ at $\phi = 0.6$ (Figs. 5 and 6). The "net branching factor" cannot be quantified from these global measurements in the rapid compression machine. However, the proportion of alkyl radicals from each reactant that eventually contribute to the low temperature chain branching channels can be derived from numerical simulations [24].

CONCLUSIONS

A major feature of the present work is the demonstration, both in the experimental results and in the supplementary modelling analysis, that considerable fuel consumption can take place prior to completion of the compression stroke when sufficiently high compressed gas temperatures are reached, not only in the present system but also, by implication, in other machines with comparable or slower compression rates. When knock occurs in a spark ignition engine (at < 2000 revs min^{-1} , say, at an average piston speed of $4 - 6 \text{ m s}^{-1}$ with a stroke of $6 - 10 \text{ cm}$) there is a similar time interval during which spontaneous oxidation of the fuel + air mixture to develop appreciably, especially at high gas densities.

The model calculations show clearly that, even in conditions where no identifiable fuel consumption has been observed at the end of the compression stroke, a significant extent of chemical activity may have already developed. For example, in the high temperature compression of

n-C₅H₁₂, at the time compression is complete, although no n-C₅H₁₂ consumption is calculated (< 0.1%) or observed, C₅ radicals, such as RO₂ and QOOH, as well as C₅ alkenes and cyclic ethers are all present in excess of ppm concentrations. In this respect the fuel + air mixture is preconditioned at the end of the compression stroke, and the subsequent ignition delay is shorter than would be predicted if a truly unreacted mixture were assumed. In fact, in this case the decrease is calculated to be as much as 10%.

ACKNOWLEDGEMENT

The authors thank EPSRC for financial support. Portion of this work was carried out under the auspices of the U.S. Department of Energy by the Lawrence Livermore National Laboratory under contract No. W-7405-ENG-48.

REFERENCES

- 1 Westbrook, C.K., Pitz, W.J. and Leppard, *SAE*, paper 912314 (1991)
- 2 Griffiths, J.F., Halford-Maw, P. A. and Rose, D.J., *Combust. Flame*, 1993, **95**, 291
- 3 Chevalier, C., Pitz, W.J., Warnatz, J., Westbrook, C.K. and Melenk, H., *Twenty-fourth Symposium (International) on Combustion*, The Combustion Institute, Pittsburgh, 1992, p 93
- 4 Minetti, R., Ribaucour, M., Carlier, M., Fittschen, C. and Sochet, L.R., *Combust. Flame* 96: 201 (1994)
- 5 Minetti, R., Carlier, M., Ribaucour, M., Therssen, E. and Sochet, L.R., *Combust. Flame* 102: 248 (1995)
- 6 Curran, H.J., Pitz, W.J., Westbrook, C.K., Hisham, H.W.M. and Walker, R.W., submitted for publication (1996)
- 7 Curran, H.J., Gaffuri, P., Pitz, W.J. , Westbrook, C.K. and Leppard, W.R., *SAE*, paper 952406, (1995)

8 Park, P. and Keck, J.C., *SAE*, paper 900027 (1990)

9 Griffiths, J.F., Jiao, Q., Schreiber, M., Meyer, J. and Knoche, K.F., *Twenty-fourth Symposium (International) on Combustion*, The Combustion Institute, Pittsburgh, 1992, p 1809

10 Schreiber, M., Poppe, C., Sadat Sakak, A., Griffiths, J.F., Rose, D.J. and Halford-Maw, P.A., *SAE*, paper 932758 (1993)

11 Beeley, P., Gray, P. and Griffiths, J.F., *Combust. Flame* 39: 269 (1980)

12 Griffiths, J.F. and Hasko, S.M., *Proc. Roy. Soc. Lond.*, A393, 371 (1984)

13 Griffiths, J.F. and Perche, A, *Eighteenth Symposium (International) on Combustion*, The Combustion Institute, Pittsburgh, 1981, p893

14 Griffiths, J.F., Jiao, Q., Schreiber, M., Meyer, J. and Knoche, K.F., *Combust. Flame* 91: 209 (1992)

15 Lund, C.M., Lawrence Livermore National Laboratory report UCRL - 52504 (1978)

16 Morley, C., *Combust. Sci. Tech.* 55, 115 (1987)

17 Griffiths, J.F. , *Prog. Energy Combust. Sci.* 21, 25 (1995) 17

18 Halstead, M.P., Kirsch, L.J. and Quinn, C.P., *Combust. Flame* 30: 45 (1977)

19 Hu, H. and Keck, J.C., *Twenty-first Symposium (International) on Combustion*, The Combustion Institute, Pittsburgh, 1986, p521

20 Griffiths, J.F., Hughes, K.J., Schreiber, M. and Poppe, C., *Combust. Flame* 99: 533 (1994)

21 Fish, A., Haskell, W.W. and Read, I.A., *Proc. Roy. Soc. Lond.*, A313, 261 (1969)

22 Mohamed C. and Pan, J., unpublished results

23 Kwok, E.S.C. and Atkinson, R., *Atmospheric Environment* 29, 1685 (1995)

24 Curran, H.J., Pitz, W.J. and Westbrook, C.K., to be published

LEGENDS TO FIGURES

- 1 Fractional extent of consumption of $n\text{-C}_5\text{H}_{12}$ at $\phi = 1$ during two-stage ignition following rapid compression to $T_C = 750 \pm 5 \text{ K}$. The error bars represent variations in results from multiple analyses of each sample collected in the cold trap. Piston motion stops at 22 ms, as shown in the pressure -time record (broken line). The chemical measurements were made in a series of experiments after quenching reaction at a given time. The pressure fall associated with a typical quenching of reaction is shown at the end of the pressure record. The chemiluminescent emission accompanying the first stage of ignition is also shown (dotted line). The simulated % reactant consumption profile is shown as a solid line.
- 2 Fractional extent of consumption of $n\text{-C}_7\text{H}_{16}$ at $\phi = 1$ during two-stage ignition following rapid compression to $T_C = 750 \pm 5 \text{ K}$. The maximum pressure attained during ignition (broken line) exceeds 3.0 MPa. Other details are as given for Fig. 1.
- 3 Fractional extent of consumption of $n\text{-C}_5\text{H}_{12}$ at $\phi = 1$ during single-stage ignition following rapid compression to $T_C = 870 \pm 5 \text{ K}$. Piston motion stops at 22 ms, as shown in the pressure record (broken line). The simulated % reactant consumption profile is shown as a solid line.
- 4 Fractional extent of consumption of $n\text{-C}_7\text{H}_{16}$ at $\phi = 1$ during single-stage ignition following rapid compression to $T_C = 870 \pm 5 \text{ K}$. The broken line represents the pressure record under reactive conditions. The chain-dot line represents the pressure record of a non-reactive mixture of similar heat capacity. Other details as for Fig. 3.

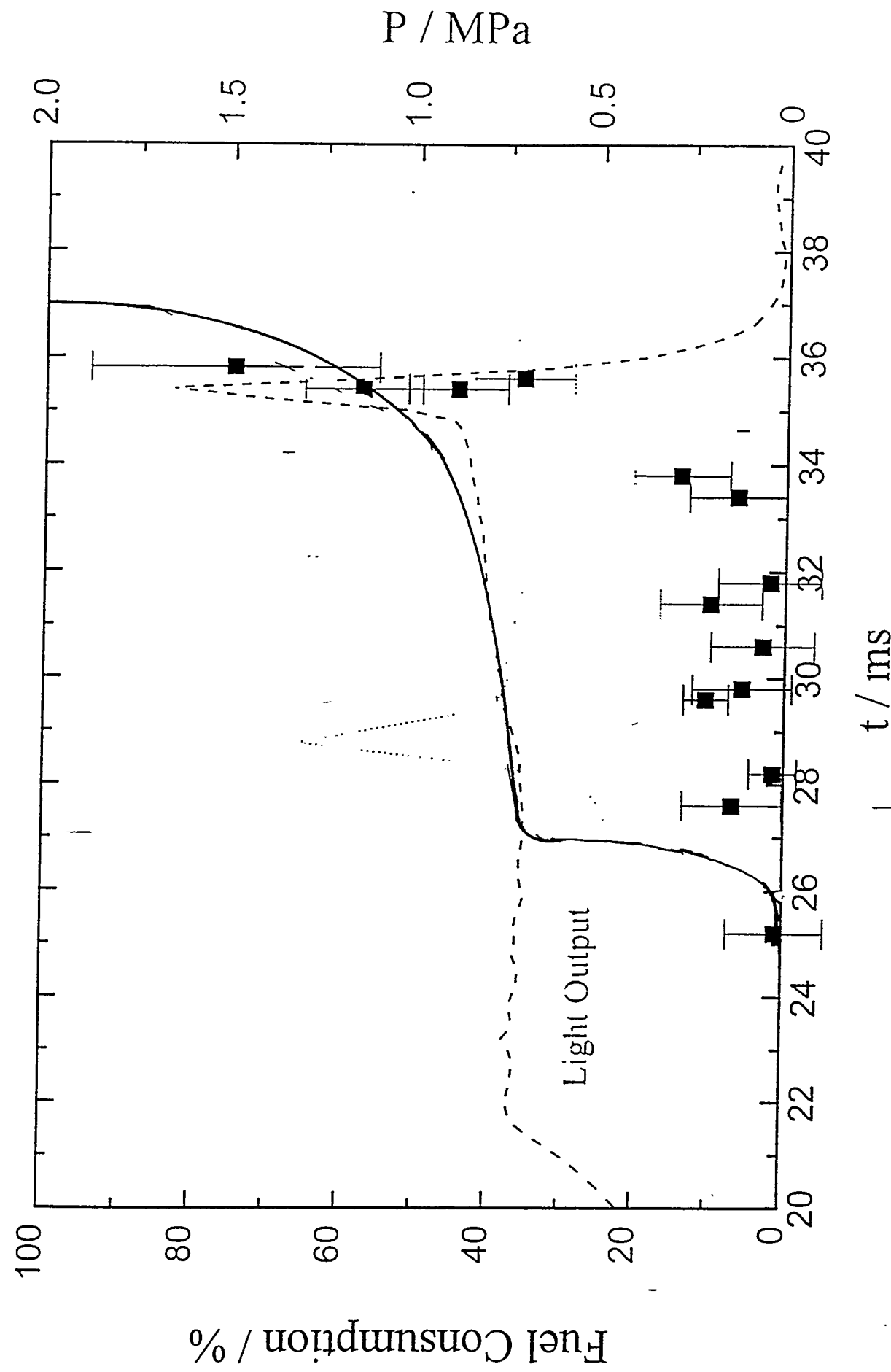
5 Fractional extent of consumption of n-C₇H₁₆ (■) and i-C₈H₁₈ (●) in a PRF 60 mixture

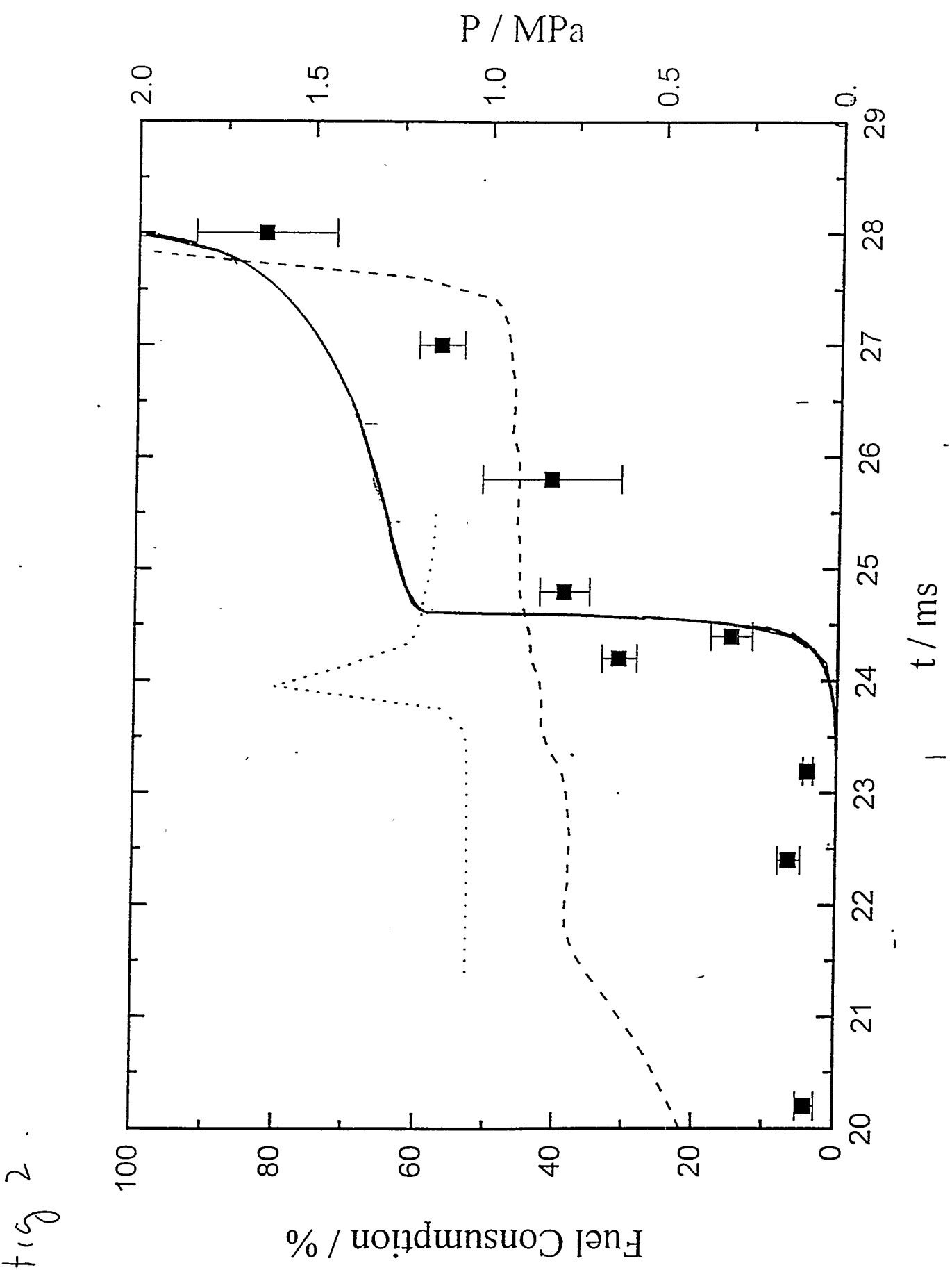
at $\phi = 1$ during single-stage ignition following rapid compression to $T_C = 860 \pm 5$ K. Error bars have been omitted from the analytical results, for clarity. They are of similar magnitude to those shown in the previous Figures. Piston motion stops at 22 ms, as shown in the pressure record. (solid line). The broken line and chain-dot line represent the simulated profiles for n-C₇H₁₆ and i-C₈H₁₈ % consumption respectively.

6. Fractional extent of consumption of i-C₈H₁₈ (●) at $\phi = 0.6$ following rapid compression to

$T_C = 860 \pm 5$ K. Piston motion stops at 22 ms, as shown in the pressure record (solid line).

Fig. 1.





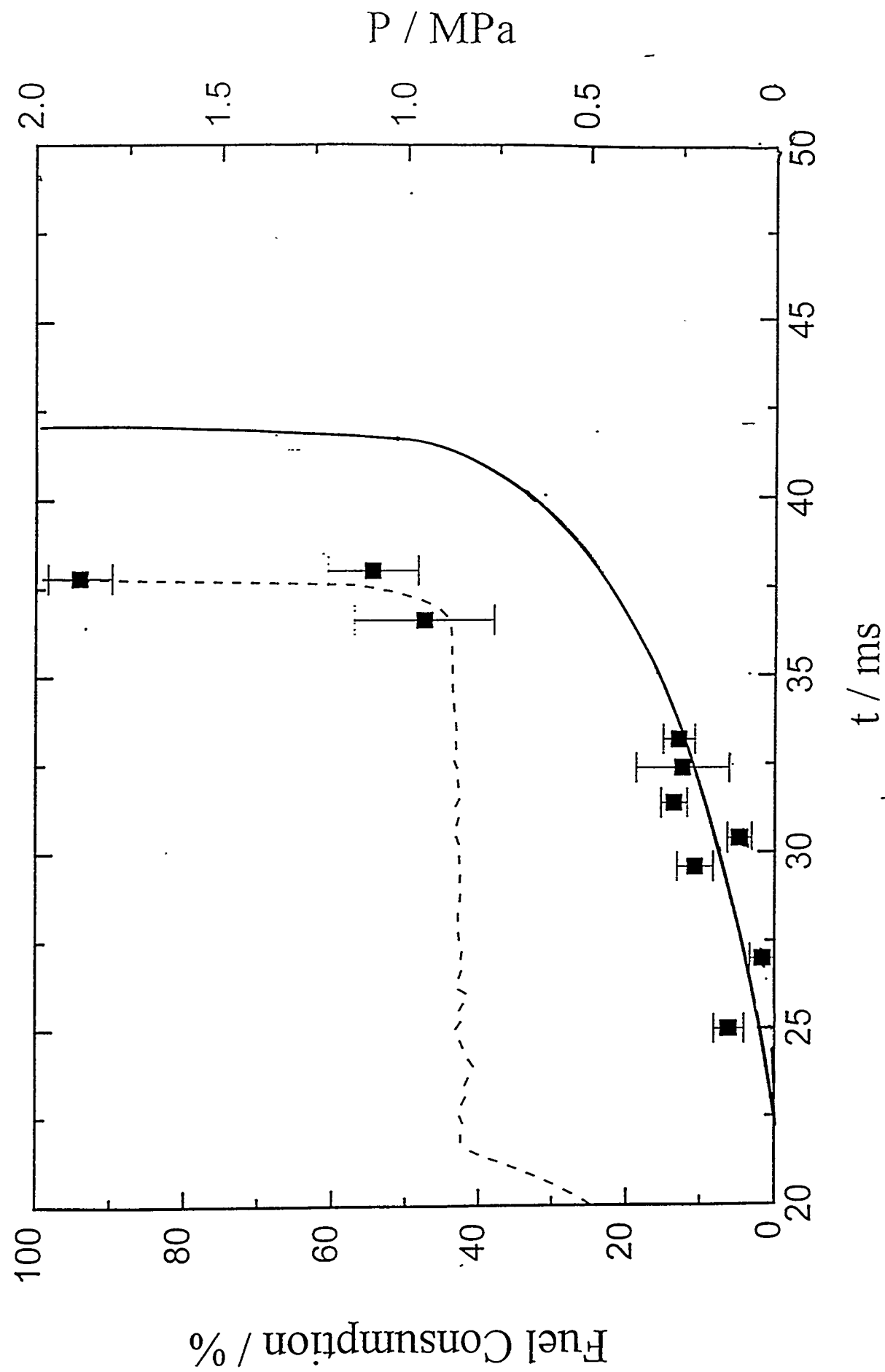
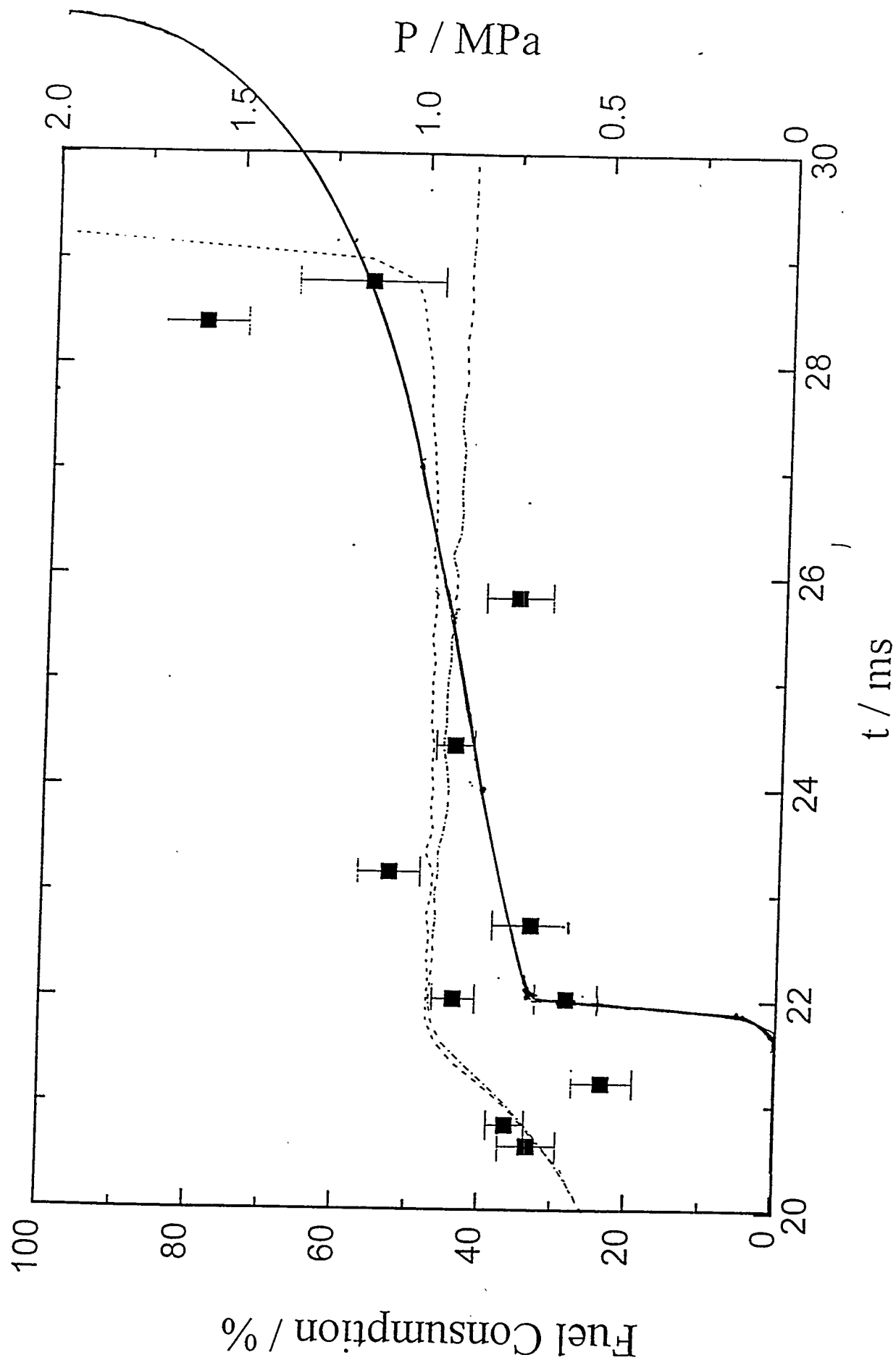
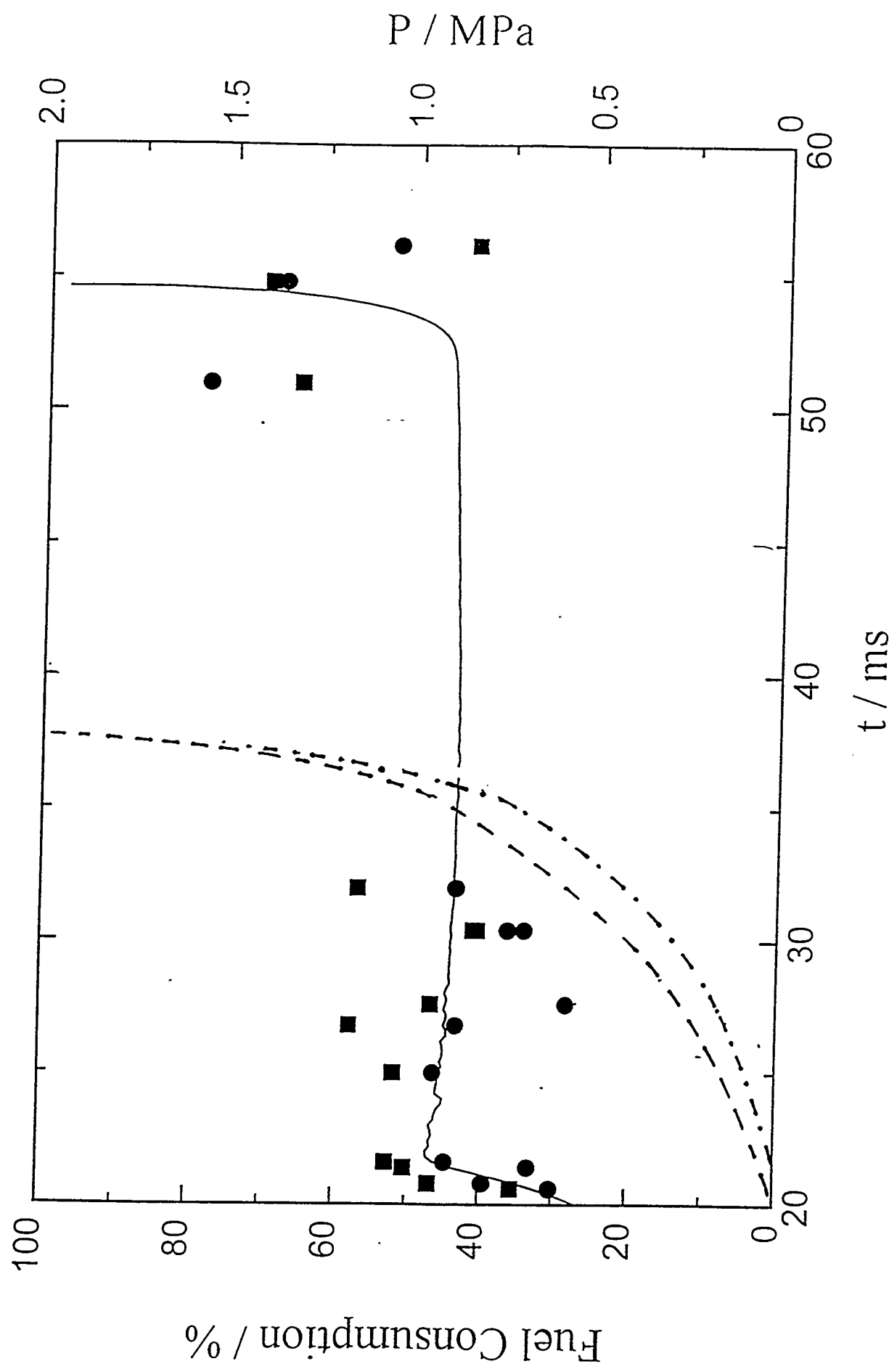


Fig. 4.





P / MPa

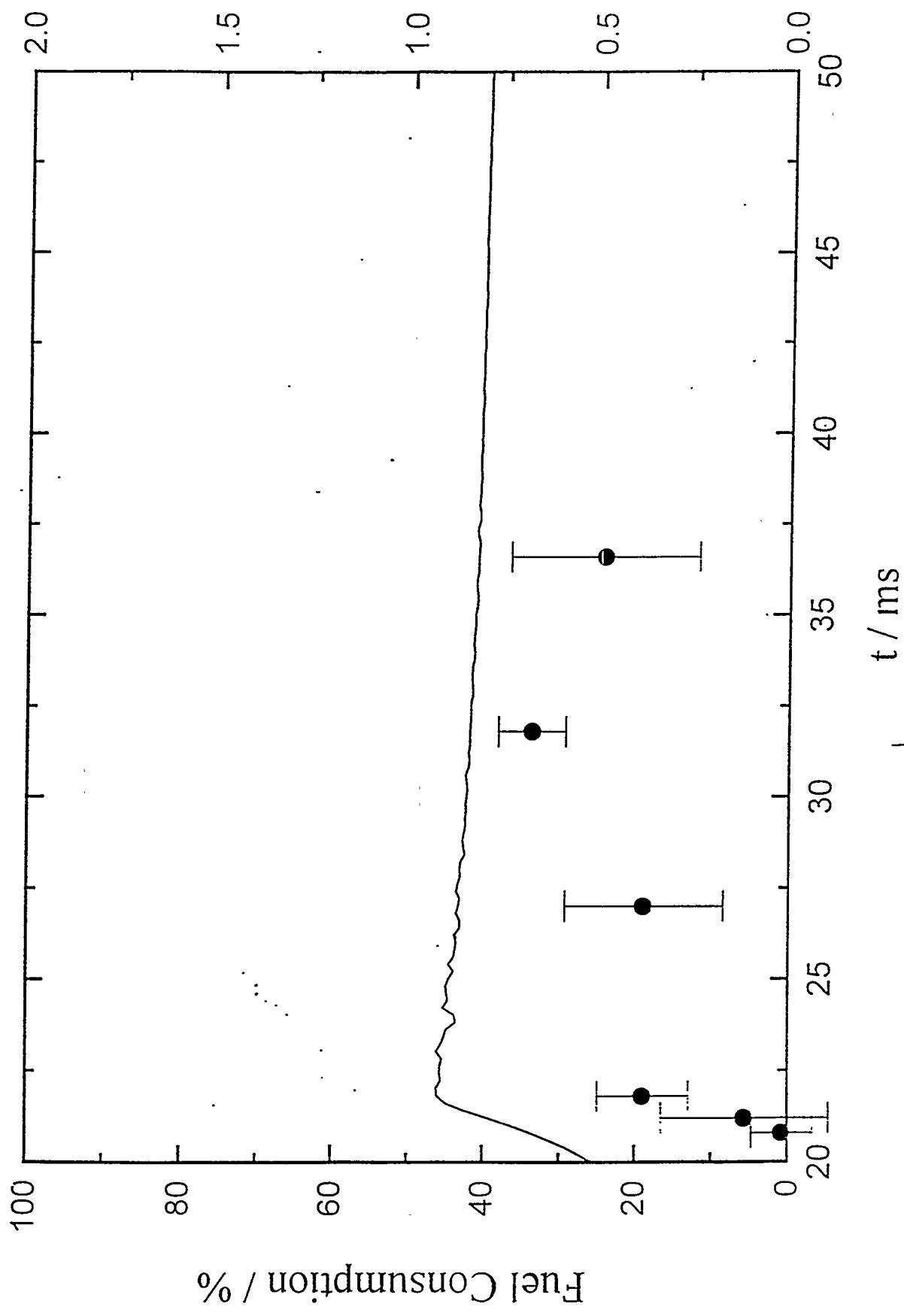


Fig. 6